



# Knickpoints and fixed points: the evolution of fluvial morphology under the combined effect of fault uplift and dam obstruction on a soft bedrock river

Hung-En Chen<sup>1</sup>, Yen-Yu Chiu<sup>2</sup>, Chih-Yuan Cheng<sup>1</sup>, and Su-Chin Chen<sup>1,3</sup>

<sup>1</sup>Department of Soil and Water Conservation, National Chung Hsing University, Taichung 40227, Taiwan

<sup>2</sup>Department of Geography, National Changhua University of Education, Changhua 50074, Taiwan

<sup>3</sup>Innovation and Development Center of Sustainable Agriculture,  
National Chung Hsing University, Taichung 40227, Taiwan

**Correspondence:** Su-Chin Chen (scchen@nchu.edu.tw)

Received: 18 February 2023 – Discussion started: 30 March 2023

Revised: 19 September 2024 – Accepted: 14 October 2024 – Published: 3 December 2024

**Abstract.** Rapid changes in river geomorphology can occur after being disturbed by external factors like earthquakes or large dam obstructions. Studies documenting the evolution of river morphology under such conditions have advanced our understanding of fluvial geomorphology. The Dajia River in Taiwan presents a unique example of the combined effects of a coseismic fault (the 1999  $M_w$  7.6 Chi-Chi earthquake) and a dam. As a result of the steep terrain and abundant precipitation, rivers in Taiwan have exhibited characteristic post-disturbance evolution over 20 years. This study also considers two other comparative rivers with similar congenital conditions: the Daan River was affected by a thrust fault Chi-Chi earthquake as well, and the Zhuoshui River was influenced by dam construction finished in 2001. The survey data and knickpoint migration model were used to analyze the evolution of the three rivers and propose hypothesis models. Results showed that the mobile knickpoint migrated upstream under the influence of flow, while the dam acted as a fixed point, leading to an increased elevation gap and downstream channel incision. Thereby, the narrowing and incision of the Dajia River began at both ends and progressively spread to the whole reach under the combined effects.

## 1 Introduction

Natural tectonic movements and artificial structures are the main factors that disturb river sediment equilibrium (Whipple and Tucker, 2002; Lang et al., 2003; Dotterweich, 2008; Cook et al., 2013; Hoffmann, 2015). These external influences often interact complexly; therefore, distinguishing between anthropogenic and natural drivers of landscape evolution is difficult. In addition, changes in these external conditions in turn drive adjustments in the riverbed, generating new landscape patterns. River morphological development generally reflects the geology and flow stress conditions (Lyell Sir, 1830). When a substantial external impact occurs, a knickpoint (a localized discontinuity in the longitudinal profile of the riverbed) often forms (Holland and Pickup, 1976), varying in size from a single water-

fall to stretches spanning several kilometers (Holland and Pickup 1976; Crosby and Whipple, 2006). These features may develop due to natural events such as extreme weather, sea level fall, and earthquake-induced surface rupture (Seidl and Dietrich, 1992; Whipple, 2004; Bishop et al., 2005; Heijnen et al., 2020).

The active fault causes a prominent knickpoint in a stream, known as tectonic uplift, leading to a local increase in channel steepness (Hayakawa et al., 2009; Huang et al., 2013; Cook et al., 2013). The abrupt elevation change in the riverbed divides the river profile into two reaches with differing slopes, altering the base level of fluvial erosion. The increasing flow stress erodes the knickpoints, causing it to migrate upstream over time. The migration process and speed are highly variable and depend on the tectonic and physical nature of the riverbed (Whipple and Tucker, 2002; Whipple,

2004). However, the fluvial response to knickpoint retreat and upstream migration requires a long duration (Howard et al., 1994; Tomkin et al., 2003), often accompanied by the cutting of a narrow channel and even the formation of a canyon. Therefore, extensive studies have been performed and tend to explore the formation and migration of knickpoints due to increases in elevation and relief (Whipple, 2001; Whipple and Tucker, 2002; Crosby and Whipple, 2006; Clark et al., 2005; Ahmed et al., 2018).

Anthropogenic factors, such as reservoir construction, are some of the most common ways humans interfere with river hydrology and sedimentation (Magilligan and Nislow, 2005; Petts and Gurnell, 2005; Graf, 2006; Nelson et al., 2013; Liro, 2017, 2019; Zhou et al., 2018). A dam, as a fixed point in the river, influences two critical components of river geomorphology: the sediment transport capacity of the flow and the oncoming sediment load (Williams and Wolman, 1984). The self-adjustment mechanisms of river channels responding to insufficient or excess sediment (Brandt, 2000) result in the change in cross-section geometry, bed material size, river pattern (Leopold and Wolman, 1957), and slope. Previous studies on the evolution of areas downstream of dams have primarily analyzed changes in downstream sandbars over large spatial scales (Horn et al., 2012; Słowik et al., 2018; Kong et al., 2020) or the ecology of the lower reaches in front of dams (Kingsford, 2000; Braatne et al., 2008; Shafroth et al., 2016). Few studies of exposed bedrock have been based on long-term observations (Inbar, 1990). In most cases, a dam effectively traps the sediment supply from the watershed. If sediment transfer to the downstream reaches of the dam is reduced, the armor layers of the riverbed are lost, which may cause an incision of the fluvial channel (Surian and Rinaldi, 2003). This incision subsequently narrows the river cross-sections and lowers the thalweg level.

Decades or hundreds of years are generally required for a riverbed to reach a new equilibrium after disturbance by external conditions, so it is difficult to understand such changes based on short-period observational data (Howard et al., 1994; Tomkin et al., 2003). Because of the abundant rainfall brought by typhoons and monsoons, the river terrain in Taiwan can alter dramatically over a short period of time. Moreover, dams in Taiwan are built primarily in steep reaches, enhancing the rapid, remarkable morphological evolution of the downstream reaches. The Chi-Chi earthquake in 1999 caused the offset of the Chelungpu thrust fault in central Taiwan (Lin et al., 2001; Ota et al., 2005). The surface rupture and uplift induced the formation of knickpoints and river gorges. After 20 years, the undercutting trend of the active channel below dams and the migration of post-earthquake knickpoints have caused the rivers to evolve into their present forms. This rapid evolution of river morphology over a short period makes Taiwan rivers suitable for case studies. The Dajia River is a unique example, as a dam structure and coseismic uplift impact it simultaneously in a short reach. The current work aims

to clarify the river changes caused by the earthquake and a dam, and to propose a hypothesis for the evolution model. To compare the various morphological developments under different external conditions, the Daan, Zhuoshui, and Dajia rivers in central Taiwan are considered in this study.

## 2 Study area, materials, and methods

The longitudinal changes in the riverbed and the accompanying river pattern changes are the objects of observation. A common type of longitudinal profile development for knickpoint retreat is illustrated in Fig. 1a (Gardner, 1983; Whipple and Tucker, 1999; Crosby and Whipple, 2006; Bressan et al., 2014). As the base level of erosion fell, the stream encountered an abrupt shift in slope from gentle to steep, which significantly accelerated the flow and subsequently led to stream bed erosion. During this process, apparent upstream degradation and downstream aggradation occurred. The knickpoint migrated upward with time accompanied by slope replacement. After the river had reached a new equilibrium in a channelized pattern, the slope replacement resulted in a natural profile. During the adjustment, the incision trend gradually slowed, and sedimentation may commence downstream (dashed line in Fig. 1a). The profile evolved from a concave curve to a graded profile (Chamberlin and Salisbury, 1904). The well-known result of dam construction is the progressive loss of the armor layer in the neighboring downstream river (Fig. 1b). The scouring baseline extended downstream of the dam (Olsen, 1999; Choi et al., 2005; Słowik et al., 2018). Because of the fixed point, the local slope at the dam toe progressively became steeper, and the dam caused the downstream river profile to be gentle and sediment transport to decrease.

Significant changes in the longitudinal profile must also be accompanied by variations in river patterns, and the interaction between fault scarps and dam obstructions within a river reach is rarely observed and studied. To address the morphological developments under different external conditions, we collected historical data (including multiyear satellite images, orthographic images, and cross-sectional and longitudinal profiles.) for three rivers in Taiwan (Daan, Zhuoshui, and Dajia), each representing the individual effects of faults and dams, as well as their combined effects.

### 2.1 Study area

Taiwan's climate is strongly affected by the western Pacific tropical cyclone. There are approximately three to four typhoons and heavy rain events yearly, and the average annual precipitation is about 2500 mm. The heavy rains during the monsoons and typhoons cause dramatic changes to riverbeds over short periods of time. In addition, because Taiwan is located at the compressive tectonic boundary between the Eurasian and Philippine Sea plates, the collision of the two continental plates causes tectonic breakage of the strata. On

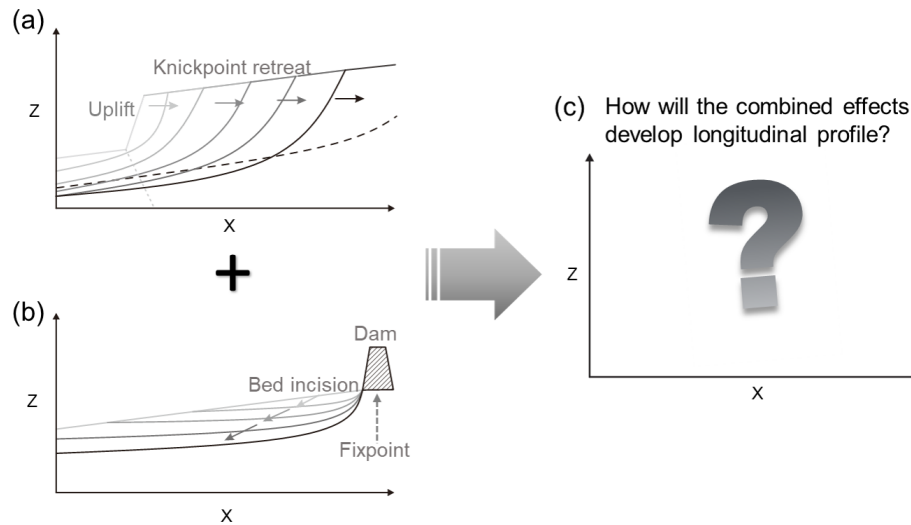


**Figure 1.** Schematic diagrams of longitudinal profile development for (a) the fault scarp's knickpoint and (b) the dam's fixed point. (c) Diagram asking the question of how the combined effects will develop in the longitudinal profile.

21 September 1999, the Chi-Chi earthquake ( $M_w = 7.6$ ) resulted in uneven uplift in the island. Three central Taiwan rivers illustrate dams or faults' effects (Fig. 2). The Daan River has been affected by vertical fault scarps, the Dajia River by both fault scarps and a dam, and the Zhuoshui River by dam obstruction. These three important rivers have very similar characteristics: their east-to-west flow direction, their range of elevation from sea level to  $\sim 3000$  m, their steep river slopes (the average slope of each river 1.5%–2.4%, Kuo et al., 2021), and their inclusion of soft rock in the mid-stream (as shown in the pink region in Fig. 2). The locations of the three rivers and the Chelungpu thrust fault are marked in Fig. 2. The southern termination of the fault crosses the Zhoushui River trending north–south. The northern termination near the Dajia and the Daan rivers shows a complex deformation pattern trending NE–SW to E–W (Lee et al., 2002) and composed of several parallel thrust faults. In the three studied reaches, the Pleistocene sedimentary rocks are mainly composed of soft rocks consisting of sandstone, siltstone, shale, and mudstone. Soft rocks have intermediate strength between soils and hard rocks, possessing unconfined compressive strengths ranging from 0.5 to 25.0 MPa (Lai et al., 2011). These rocks are generally poorly lithified and weakened by a high water content; therefore, their resistance to water erosion is poor. The riverbed rock is readily incised by flooding flow when the upper armor protective layer was lost (Huang et al., 2014).

The Chi-Chi earthquake produced a surface rupture 80 km long. Several fracture planes at the north end of the fault caused uneven uplift in the region (Lee et al., 2002). One of the ruptures passed through the right bank of the Shigang Dam (constructed in 1977) on the Dajia River, causing serious damage to the dam structure. The maximum vertical displacement of the surface rupture was 9 m, increasing the drop

height of the bed level between the face and the back of the dam markedly. The dam reconstruction was finished in 2000. The repaired Shigang Dam was intended to store  $2.4 \times 10^6$  m<sup>3</sup> of water after the Chi-Chi earthquake; however, owing to deposition in the reservoir, only  $\sim 1.4 \times 10^6$  m<sup>3</sup> of water can now be retained. After the earthquake and the reconstruction, the fluvial morphology has rapidly changed. The original armor layers on the riverbed in front of the Shigang Dam were rapidly lost, exposing the soft bedrock. The two rupture surfaces at the north end of the Chelungpu fault uplifted a 1 km reach of bed in the Daan River, with a maximum vertical uplift of 10 m.

Although the southern end of the Chelungpu fault passes downstream of the Jiji Dam (Zhuoshui River), the fault uplifted the bed level by  $\sim 2$  m, less than the uplifts in the Daan and Dajia rivers. The Jiji Dam was built in 2001 (after the 1999 Chi-Chi earthquake), is situated on the narrowest part of the Zhuoshui River, and has a maximum designed storage capacity of  $10 \times 10^6$  m<sup>3</sup>. Due to the large sediment yield in the Zhuoshui River watershed, the present-day adequate water storage capacity is only  $\sim 4 \times 10^6$  m<sup>3</sup>. The Jiji Dam downstream is known for its soft bedrock canyon features formed by dam-obstructed water scouring.

## 2.2 Data collection and analysis methods

Analysis of the effects of faults and dams, alteration of river patterns, changes in thalweg levels, and variations in river cross-sections are crucial to revealing the process of river evolution. SPOT-5 and SPOT-6 satellite images (2 m in resolution) and orthographic images (25–50 m in resolution) obtained by the Center for Space and Remote Sensing Research, National Central University (CSRSR/NCU) and the Aerial Survey Office (AFASI) of Taiwan were used to assess

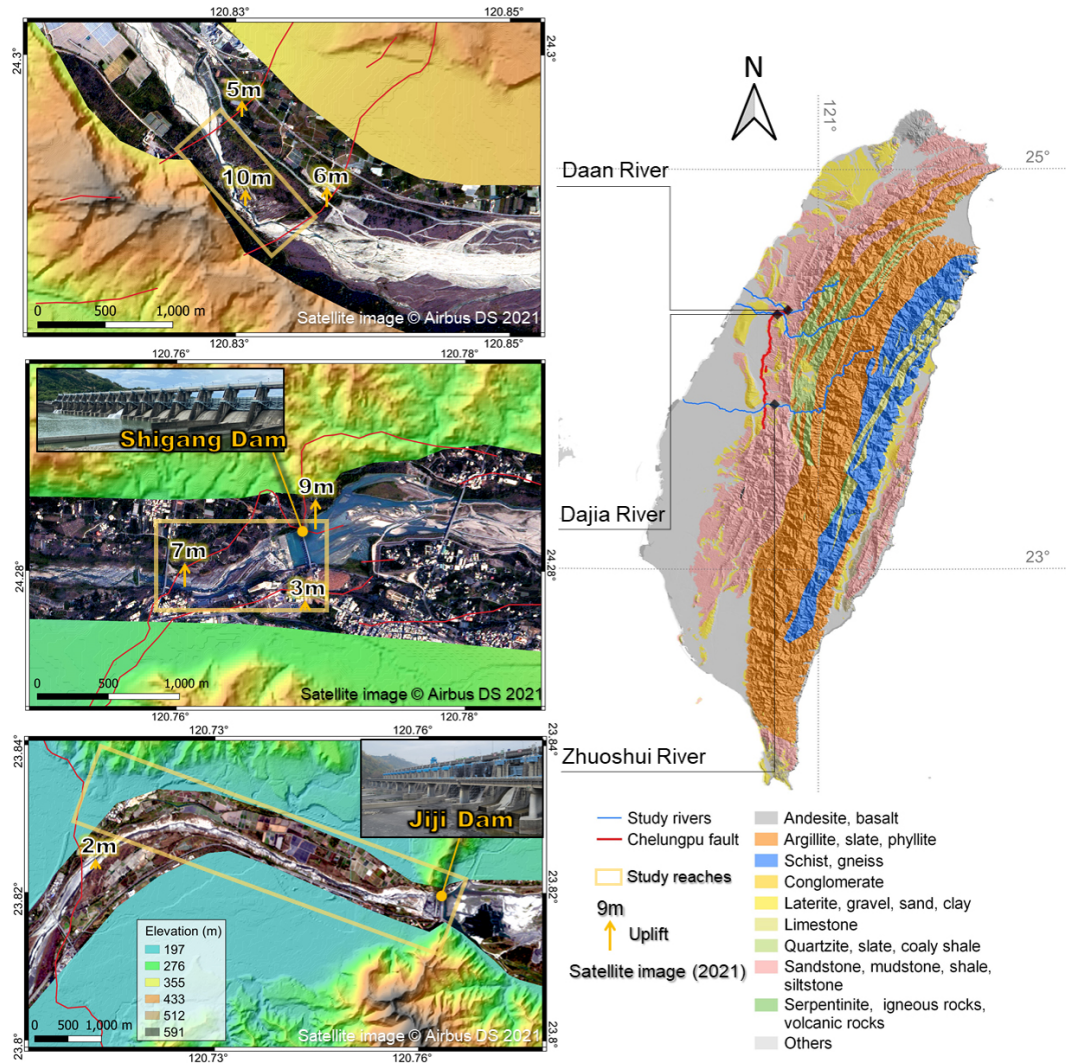


**Figure 2.** Locations of the Chelungpu fault, the three studied rivers, and satellite images (from CSRSR/NCU, 5 February 2021, 2 m resolution) showing the studied reaches.

changes in river patterns. Multiyear cross-sectional and longitudinal profiles were established from historical surveys by the Water Resources Agency (WRA). The survey was conducted using total station, GPS, and depth sounder data. The interval of survey points should be 5–10 m, and the elevation error must not exceed 5 cm. Additional analyses of knickpoint retreat and variations in river elevation and width were carried out. We also incorporated terrain data from other relevant studies into our research materials. For example, the longitudinal profiles proposed by Cook et al. (2013), which generated digital surface models (DSMs) for the years 1998 and 2004 using aerial photographs, were also included in our research materials. The locations of knickpoints were determined by identifying abrupt terrain changes and the positions of splash in the images. We also collected the daily flow data from the WRA and calculated the cumulative flow to compare the relationship between knickpoint retreat and dis-

charge. The width ( $W$ ) and depth ( $D$ ) of the river can be used to quantify changes in river patterns. In order to analyze the variation in channel width, depth, and aspect ratio ( $W/D$ ), we calculated the bankfull discharge width and depth, which represents the maximum flow that can occur in a river before water starts overflowing and spreading out onto the floodplain. We identified the river banks and extracted channel widths from orthographic images. The banks were defined as the boundaries between the main channel and the adjacent floodplain.

### 2.3 Mathematical model

The application of the mathematical model provides an abstract description of a concrete system using physical concepts and mathematical language. A one-dimensional Exner equation (Exner, 1925) is used to describe the advective and

diffusive knickpoint migration (Bressan et al., 2014):

$$\frac{\partial z}{\partial t} + \frac{1}{(1 - p_s)} \frac{\partial q_s}{\partial x} = 0, \quad (1a)$$

where  $z$  is the bed elevation along the thalweg,  $p_s$  is the porosity of bed sediment,  $t$  is the time,  $x$  is the distance,  $q_s$  is the sediment discharge per unit width that is estimated by the product of the surface height change  $\eta$ , and the knickpoint migration rate  $dx/dt$  is expressed as Eq. (1b).

$$q_s = -\eta \frac{dx}{dt} \quad (1b)$$

The migration rate as a sediment separation per unit area homogeneously distributed over the eroding surface is expressed as Eq. (1c):

$$\frac{dx}{dt} = k_d [\tau(x) - \tau_C], \quad (1c)$$

where  $k_d$  is the erodibility,  $\tau$  is the bed shear stress, and  $\tau_C$  is the critical shear stress of the bed material. The condition of an obvious knickpoint face ( $\tau$ ) should be estimated using a formula that considers knickpoint as a submerged obstacle (Eq. 1d) (Engelund, 1970).

$$\tau(x) = M\tau_0 \left[ 1 + A \frac{(z - z_0)}{H_0} + B \frac{\partial z}{\partial x} \right] \quad (1d)$$

The factors  $M$ ,  $A$ , and  $B$  in Eq. (1d) are parameters related to localized phenomena. Here,  $\tau_0$ ,  $z_0$ , and  $H_0$  are the shear stress, bed elevation, and the water depth upstream of the knickpoint, respectively. The term  $B \frac{\partial z}{\partial x}$  represents the change in shear stress due to the local slope. The shear stress in the channel section upstream of the knickpoint crest ( $\tau_0 = \gamma H_0 S_0$ , where  $\gamma$  is the specific weight of water changes across the knickpoint due to the abrupt change in bed topography (Eq. 1d). Substituting Eqs. (1b)–(1d) into Eq. (1a), Eqs. (2a)–(2c) were obtained as given below:

$$\frac{\partial z}{\partial t} - C \frac{\partial z}{\partial x} - D \frac{\partial^2 z}{\partial x^2} = 0 \quad (2a)$$

$$C = \left( \frac{\eta k_d \gamma}{1 - p_s} \right) S_0 M A \quad (2b)$$

$$D = \left( \frac{\eta k_d \gamma}{1 - p_s} \right) S_0 H_0 M B \quad (2c)$$

Here the coefficients of the first- and second-order spatial derivatives,  $C$  and  $D$ , are known as the advection and diffusion coefficients, respectively.  $C$  represents the moving speed, and  $D$  represents the diffusion constant. It can be concluded that the key controls of the knickpoint retreat are the channel slope, the erodibility of the bed of the river reach, the knickpoint face height, and the upstream water depth. The survey data could calibrate these physical parameters. Therefore, the present equation is a physical-based model

that can be solved with the second-order accurate implicit finite-difference scheme that was implemented in MATLAB. However, it is essential to recognize that the numerical model is conceptual and involves several assumptions, such as not considering variations in the horizontal 2D plane of the terrain and assuming homogeneous parameters within the simulation area. The numerical model cannot fully capture the scenario's detailed morphology and environmental conditions. It is a conceptual model based on physical mechanisms, providing trends rather than precise representations.

### 3 Results

#### 3.1 Fault effect on Daan River canyon

The scarps across the Daan River that were uplifted by the Chi-Chi earthquake caused a dramatic change in the topography, disturbing the dynamic equilibrium of the fluvial system. Cook et al. (2013) proposed that the knickpoint propagated rapidly after 2004 and pointed out that the tool effect caused pronounced fluvial incision of the bedrock after the disappearance of bedload. Knickpoint propagation was influenced by the anti-formal geological structure of the area, the presence and orientation of interbedded strong and weak lithologies, and the proportion of discharge entering the main channel. Huang et al. (2013) also proposed that the knickpoint retreat rate can be affected by several factors, including discharge, rock properties, geological structures, and bedrock orientation. The channel development of the studied reach and the behavior of knickpoint retreat were assessed by analyzing multiyear data related to the form and cross-section of the river.

Successive orthographic images of the studied reach of the Daan River from 2000 to 2017 and the corresponding flow paths are illustrated in Fig. 3. River cross-sections constructed from precise survey data are provided in Fig. 4. Chronological longitudinal profiles of the river reach are shown in Fig. 5. Longitudinal profile data from Cook et al. (2013) were included to make information more complete. The effect of the earthquake on the surface elevation is clearly visible in Fig. 5. In addition to the survey data, the advective and diffusive knickpoint migration model (Eq. 2) was solved to mathematize the knickpoint retreat progress after the Chi-Chi earthquake. The initial condition and boundary condition are needed to solve the equation. The initial condition is the longitudinal profile in 1999, while the boundary conditions are the real bed changes in the upstream and downstream boundaries. The  $C$  and  $D$  are physical parameters and were calibrated by the survey data. In Eq. (2),  $C$  represents the moving speed, while  $D$  represents the diffusion constant. These two coefficients reflect the rate of bed erosion, which is physically composed mainly of bed shear stress (Eq. 2b and c). Due to the actual bed erosion rates varying with time, the parameters were adjusted to match the real changes. Before 2004,  $C$  was  $22.0 \text{ m yr}^{-1}$  and  $D$  was

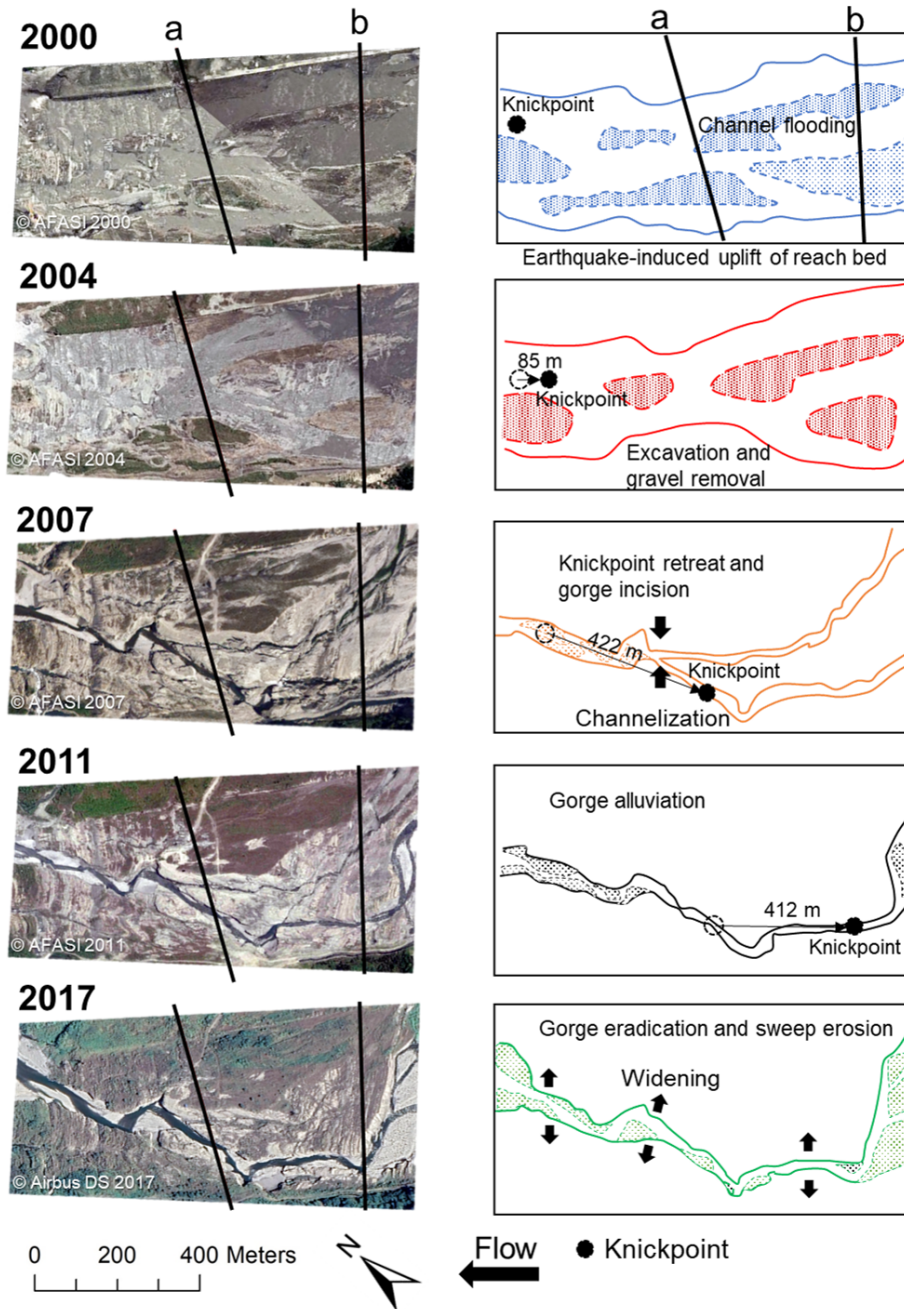


**Figure 3.** Orthographic images (2000–2011), satellite image (2017), and flow paths of the studied reach of the Daan River from 2000 to 2017.

$10.0 \text{ m}^2 \text{ yr}^{-1}$ ; after 2004,  $C$  was  $91.5 \text{ m yr}^{-1}$  and  $D$  was  $18.5 \text{ m}^2 \text{ yr}^{-1}$ . The simulation was continued until 2011 when the knickpoint disappeared. The result of the modeling is shown in the top-left corner of Fig. 5. The knickpoint progressively retreats accompanied by slope replacement. The variation trend of the simulation and survey data is generally consistent, and the speed ( $C$ ) has a larger value in 2004–2011, which is also consistent with the observation.

The long-term development of the studied reach of the Daan River in the past 20 years, after the coseismic uplift,

can be divided into three periods: downstream erosion and slow knickpoint migration (earthquake to 2004), sudden migration of the knickpoint (2004–2011), and gorge widening and eradication (2011–present).

### 3.1.1 Downstream erosion and slow knickpoint migration (earthquake to 2004)

After the Chi-Chi earthquake, coseismic ground deformation created a pop-up obstruction across the river, forming

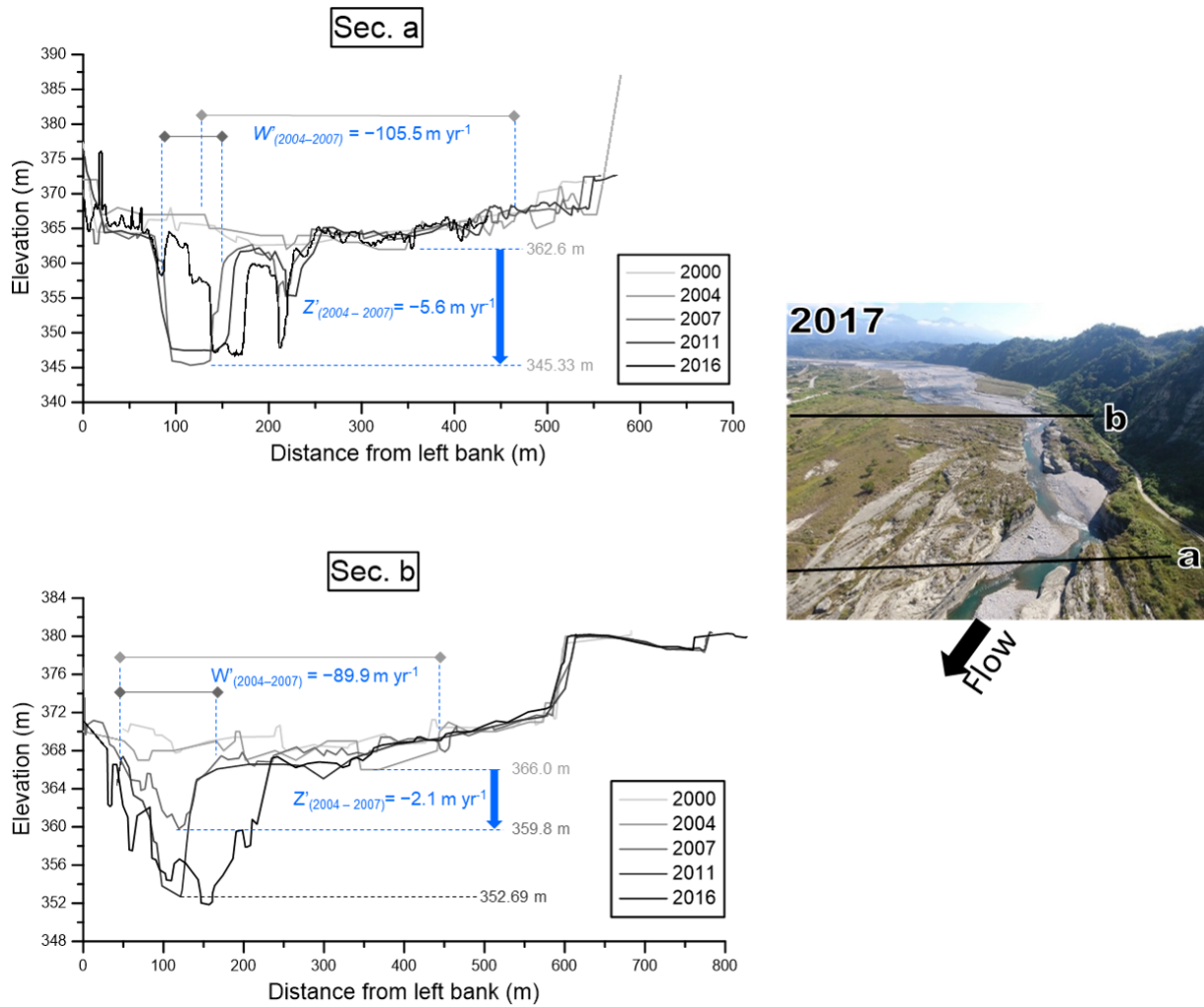


Figure 4. Cross-sections a and b of the Daan River from 2000 to 2016 (from the WRA).

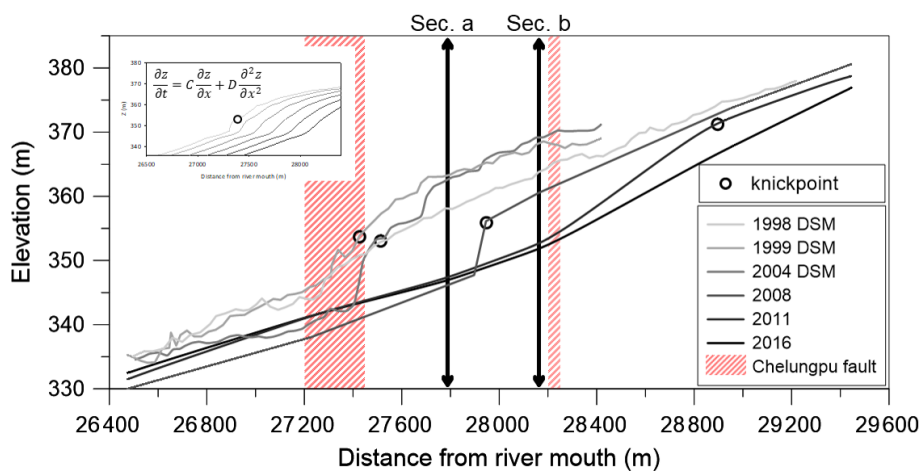


Figure 5. Longitudinal profiles of the studied reach of the Daan River from 2000 to 2016. Profiles for 1998–2008 are from Cook et al. (2013), and those for 2011–2016 are from the WRA. Data between 1998 and 2004 are derived from aerial-photograph-generated DSM. The subfigure shows the simulated knickpoint retreats using the advective-diffusive model at the top left.

a barrier lake behind the rupture scarp. The obstacle blocked the river flow and trapped the sediment, causing the riverbed downstream of the rupture scarp completely lose the armor layer. When the armor layer was lost, bedrock incision occurred downstream of the uplifted zone, and the knickpoint retreat appeared. On the other hand, no significant erosion occurred between cross-sections a and b during that period (Figs. 3 and 4). A comparison of the cross-sections for 2000 and 2004 (Fig. 4) reveals that most parts of the section a even experienced deposition. Slight erosion in some places can be detected in the longitudinal profiles (Fig. 5) between 1999 (after the earthquake) and 2004. Although the seismic uplift produced an obvious knickpoint on the riverbed, it migrated only slightly (85 m; Table 1) between 2000 and 2004. The downstream reach of the uplifted zone showed evidence of scour, but no noticeable bedrock incision or canyon landscape had developed yet.

### 3.1.2 Sudden migration of knickpoint (2004–2011)

The orthographic image for 2007 (Fig. 3) clearly shows that the armor layer had been removed, the bedrock had been exposed, and the deep incision had formed a narrow channel. The knickpoint retreated upstream by approximately 422 m between 2004 and 2007, accompanied by continued scouring downstream. In the uplifted reach, under the stress of the concentrated flow in the newly formed channel, the tool effect resulted in a deepened incision of the rock bed, and a canyon landform gradually developed. In the 2007 cross-section data for section a, a canyon close to the left bank can be observed, which persisted until 2011. A rapid incision rate ( $5.6 \text{ m yr}^{-1}$ ) occurred in section a, which also experienced a narrowing rate of about  $105.5 \text{ m yr}^{-1}$ . Bed incision and narrowing of the main channel occurred in section b simultaneously, with a narrowing rate of approximately  $89.9 \text{ m yr}^{-1}$  and an incision rate of about  $2.1 \text{ m yr}^{-1}$ . Between 2007 and 2011, the knickpoint retreated upstream by about 412 m; the incision at section a was lessened, but section b experienced a notable incision into the rock bed accompanied by knickpoint retreat. Because an obvious gorge channel had appeared in the uplifted zone, sediment from upstream was transported downstream, and downstream scouring transformed gradually into sedimentation; therefore, the convex longitudinal profile was gradually erased.

### 3.1.3 Gorge widening and eradication (2011–present)

After 2011, the knickpoint became insignificant in the longitudinal profile, meaning that the thalweg scouring trend slowed. The morphology development is dominated by lateral erosion instead of vertical incision. The narrow, deep canyon evolved into a U-shaped canyon with a wide bottom. River pattern migration from upstream caused the canyon-type channel to commence transforming into a braided channel. The main channel of section a experienced deposition

as a result of the sediment supply being adequate (Fig. 5). Cook et al. (2014) proposed a mechanism of gorge eradication, called downstream sweep erosion, which rapidly transformed the gorge into a beveled floodplain through the downstream propagation of a wide erosion front located where the broad upstream channel abruptly became a narrow gorge. The sweep boundary is clearly visible in the orthographic images for 2011 and 2017 (Fig. 3). Additional large floods are expected to cause a marked widening of the channel instead of deepening (Huang et al., 2013). It has been estimated that removal of the gorge erosion will take 50 years (Cook et al., 2014).

Significant incision of the channel is common after a riverbed has been uplifted suddenly by tectonic movement and the bed slope changes dramatically (Merritts and Vincent, 1989). This was the case for the Daan River after the Chi-Chi earthquake. After the coseismic uplift, the base level of erosion downstream reduced, meaning that erosion increased. The river width became notably narrower and deeper. Upward movement of the knickpoint caused the river channel in the uplifted section to narrow rapidly. The concentrated flow caused a rapid incision of a weak geological layer in the riverbed, meaning that the channel width decreased sharply. Therefore, the uplifted section formed a canyon landform. As the slope at the knickpoint gradually recovered, the incision slowed, and sediment transport down the recovered river resulted in sediment deposition in the downstream channel. The river also gradually developed lateral erosion upstream, and the river channel tended to widen. The channelization is expected to have been swept because the sweep boundary migrated progressively downward.

## 3.2 Jiji Dam effect on Zhoushui River

Construction of the Jiji Dam on the Zhoushui River began in 1996, and it began operation in 2001. Orthographic images; flow paths of the studied reach; and the locations of cross-sections c, d, and e below the Jiji Dam for 1998 to 2018 are provided in Fig. 6. Chronological survey data of cross-sections c, d, and e are provided in Fig. 7. Chronological longitudinal profiles of the studied reach are illustrated in Fig. 8. The river is located at the southern termination of the Chelungpu fault (Fig. 1), where the elevation gap caused by the earthquake is relatively small. In 1998, the Zhoushui River was a broad and braided river, with many sandbars downstream of the dam (Fig. 6). In 2003, 2 years after dam operation had commenced, the riverbed armor layer had been lost, and the exposed soft bedrock was clearly visible within 700 m of the toe of the dam because of a lack of sediment. The bedrock's incision deepened due to the tool effect, and the flow path concentrated gradually in front of the dam. From 2003 to 2007, the effect zone gradually expanded, and exposed bedrock extended to  $\sim 3.2 \text{ km}$  downstream of the dam. Between 2007 and 2018, the channelization and the zone with exposed bedrock expanded continuously to 6.5 km



**Table 1.** Characteristics of the studied reaches of the Daan, Zhuoshui, and Dajia rivers.

River	Time interval	Section	Bed change		Channel widening		Knickpoint retreat		C (m yr <sup>-1</sup> )
			(m)	(m yr <sup>-1</sup> )	(m)	(m yr <sup>-1</sup> )	(m)	(m yr <sup>-1</sup> )	
Daan	2000–2004	a	-0.60	-0.15	-103.77	-25.94	85	21.25	22
		b	-1.76	-0.44	47.50	11.88			
	2004–2007	a	-16.67	-5.56	-316.50	-105.50	422	140.67	
		b	-6.20	-2.07	-269.82	-89.94			
	2007–2011	a	2.06	0.52	19.30	4.83	412	103.00	
		b	-7.11	-1.78	-64.19	-16.05			
	2011–2016	a	-0.45	-0.09	31.19	6.24	-	-	
		b	-0.84	-0.17	41.27	8.25			
Zhuoshui	1998–2008	c	-0.46	-0.05	-96.22	-9.62	-	-	
		d	-2.24	-0.22	-130.41	-13.04			
		e	-11.59	-1.16	-246.32	-24.63			
	2008–2012	c	-5.44	-1.36	-258.44	-64.61	-	-	
		d	-2.77	-0.69	18.43	4.61			
		e	3.00	0.75	5.22	1.31			
	2012–2015	c	-4.46	-1.49	-171.56	-57.19	-	-	
		d	-6.65	-2.22	-133.24	-44.41			
		e	-4.94	-1.65	-73.11	-24.37			
	2015–2018	c	-0.84	-0.28	13.57	4.52	-	-	
		d	-0.86	-0.29	1.31	0.44			
		e	-3.03	-1.01	8.70	2.90			
Dajia	2000–2005	f	-2.39	-0.48	-14.12	-2.82	40	8.00	
		g	-2.02	-0.40	-116.44	-23.29			
	2005–2008	f	-2.57	-0.86	-39.90	-13.30	186	62.00	
		g	-7.50	-2.50	-142.97	-47.66			
	2008–2014	f	-1.33	-0.22	12.28	2.05			
		g	-0.38	-0.06	2.21	0.37			
	2010–2014	h	-4.20	-1.05	-25.45	-6.36	219	24.33	
	2014–2017	f	-1.39	-0.46	-10.44	-3.48			
		g	-3.32	-1.11	8.84	2.95			
		h	-5.27	-1.76	-20.63	-6.88			

downstream of the dam. Due to the channelization, the river cross-section became narrow and deep.

The transformation of the river and the rates of lateral and vertical change are clearly visible in the river cross-sections (Fig. 7). There was no apparent erosion of section c in 2008, but the sections closer to the dam (d and e) exhibited obvious incision (Fig. 7). After the loss of the riverbed armor layer, the flow cut down into weak bedrock. The deep main channels' development is clearly visible in sections d and e between 1998 and 2008. During this time, the incision rate of section e was around 1.2 m yr<sup>-1</sup>, and the narrowing rate was around 25 m yr<sup>-1</sup>. During 2008–2012, engineering measures were installed: between section d and sec-

tion e, groundfills, spur dikes, and tetrapods were added to the river channel to prevent erosion, and the riverbed level rose slightly at section e. However, the channel width of section c was markedly narrower, with a narrowing rate of roughly 65 m yr<sup>-1</sup>. Between 2008 and 2015, sections c and d incision rates were roughly 1.4 m yr<sup>-1</sup>. Progressive layer-by-layer erosion is apparent in the chronological longitudinal profiles (Fig. 8). Incision of the studied reach became increasingly severe: incision commenced at section e and subsequently extended downstream to sections d and c. We infer that headward erosion did not dominate the riverbed because the Chelungpu fault passed through the river some distance from the dam and caused only 2 m of uplift. In contrast, dam-

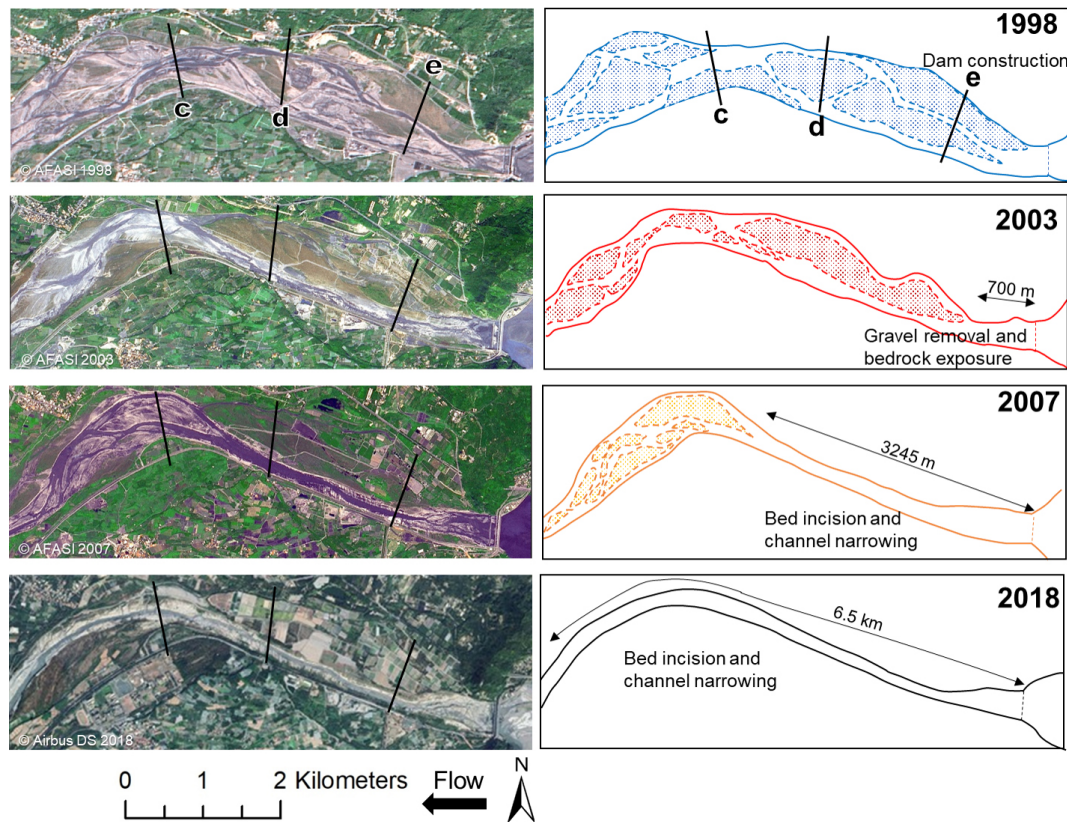


**Figure 6.** Orthographic images (1998–2007), satellite image (2018), and flow paths of the studied reach of the Zhuoshui River from 1998 to 2018.

induced downward incision of the riverbed caused degradation of the reach. There is an approximately 15 m difference between the bed level of 1998 and that of 2018.

### 3.3 The combined effect of Shigang Dam and fault on Dajia River

The studied reach of the Dajia River, which lies downstream of the Shigang Dam, was affected by both the dam and uplift caused by the Chi-Chi earthquake. The Shigang Dam was broken by uneven uplift of the fault scarp across the dam (9 m on the right side and 3 m on the left), and the downstream section f rose by  $\sim 7$  m (see Fig. 2). The earliest knickpoint formed close to section f and moved headward with time. During 2000–2005, the knickpoint retreated by  $\sim 40$  m, and another new knickpoint formed between sections g and h (Fig. 9) under the co-effect of river pattern changes and bed rock differential erosion. The damming effect of the Shigang Dam also caused the armor layer to be removed. The bedrock became exposed shortly after the earthquake; however, section f was obviously incised during 2000–2005, whereas incision of section g did not occur until 2005–2008 (Fig. 10). Between 2000 and 2005, engineering measures were installed on several occasions to mitigate the

obvious erosion. The river pattern between section g and the dam was braided during the period.

The incision rate of section g was  $\sim 1.1 \text{ m yr}^{-1}$  during 2005–2008, and the narrowing rate was  $\sim 47.7 \text{ m yr}^{-1}$ . During the same time interval, the downstream knickpoint (between sections f and g) disappeared due to river training in 2008. The knickpoint between section g and section h retreated rapidly toward the dam (Figs. 9 and 11). During 2005–2008 and 2008–2017, the knickpoints moved upstream by approximately 186 and 219 m, respectively. This retreat of the knickpoints implies that river channel scouring did not stop. Because the riverbed strata trend northeast–southwest, flow-scouring preferentially deepened the left part of the rock bed, which moved the channel closer to the left bank. After 2008, the flow channel extended closer to the toe of the dam. Due to the severe incision, the government started surveying section h after 2010 (Fig. 10). Significant bedrock incision was recorded, with an incision rate of  $\sim 1.4 \text{ m yr}^{-1}$  at section h during 2010–2017. In 2008, it can be observed that the knickpoint existed in the reach between sections g and h; therefore, the slope of the channel is still discontinuous. The 2017 photograph shows a single, meandering channel that starts from the dam and runs through sections h and g, eventually reaching section f, where the knickpoint had initially

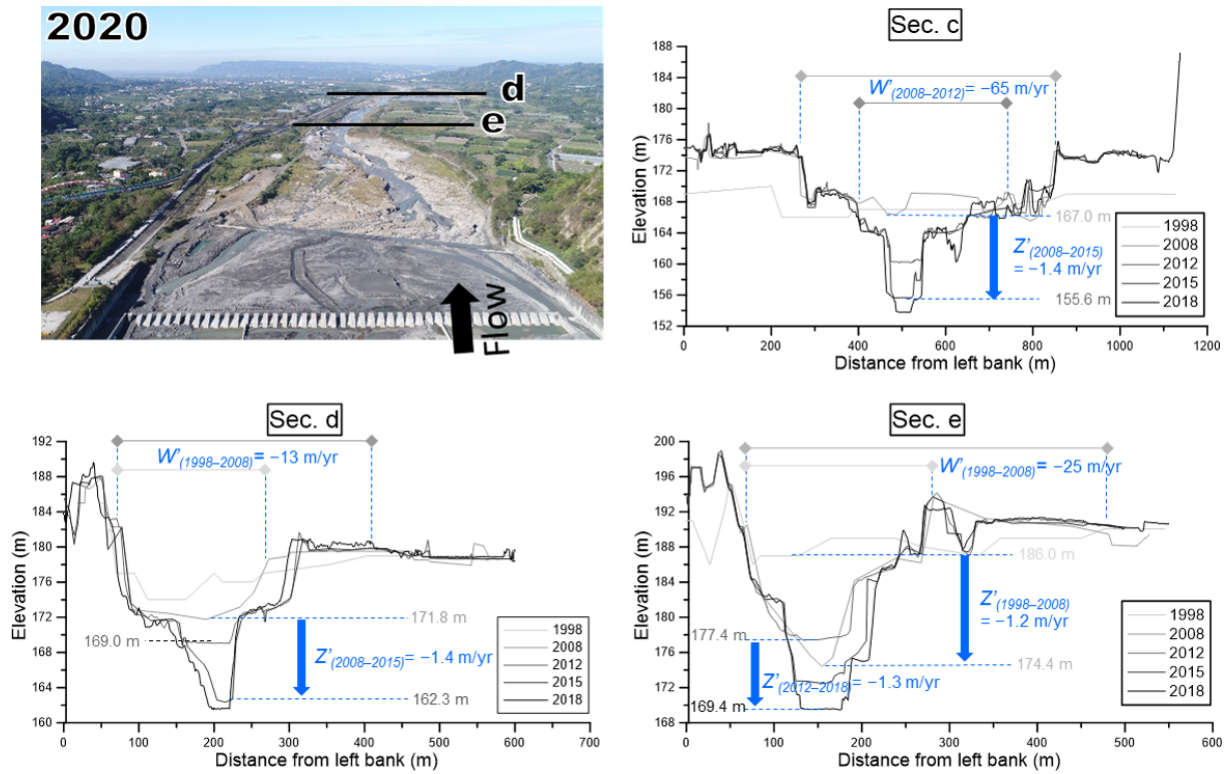


Figure 7. Profiles of cross-sections c–e of the Zhuoshui River from 1998 to 2018 (from the WRA).

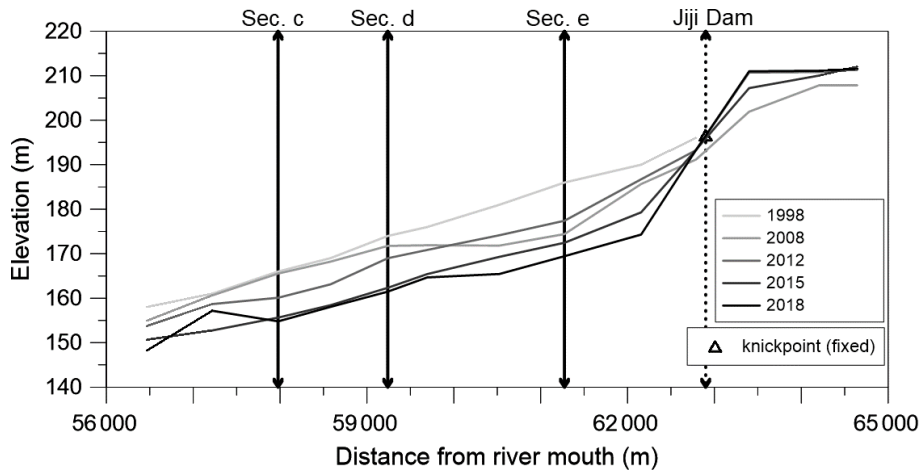
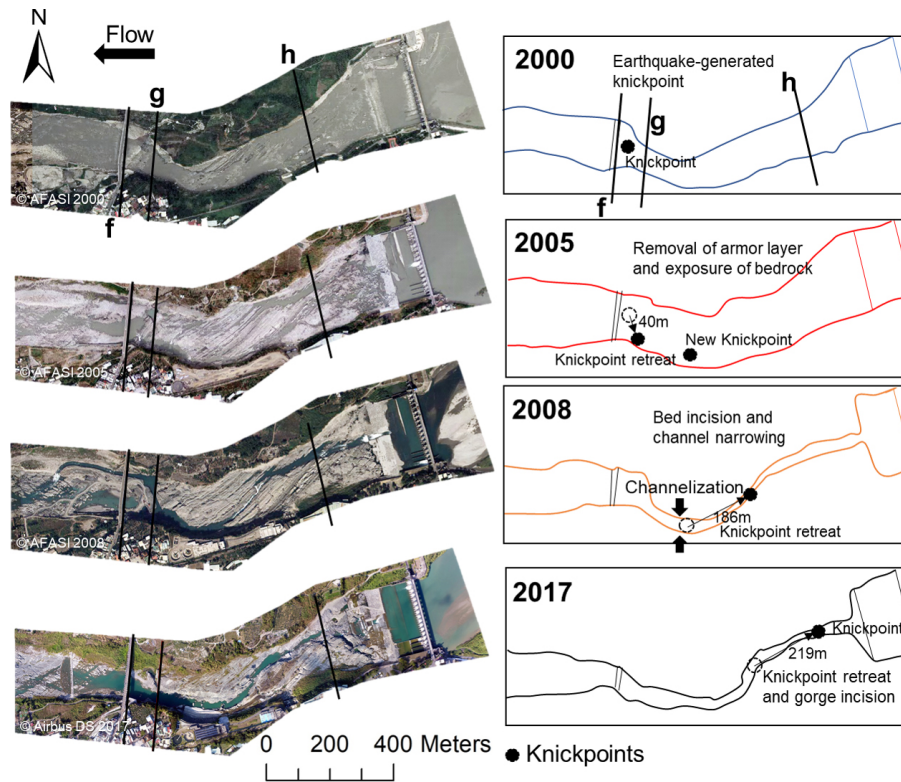


Figure 8. Longitudinal profiles of the studied reach of the Zhuoshui River from 1998 to 2018 (from the WRA).

formed (Fig. 10). Overall, the area downstream of the Shigang Dam displayed headward erosion of the knickpoint and incision of the rock bed in front of the dam.

In the Dajia River, the advection and diffusion equation (Eq. 2) was also used to represent the variation mode of knickpoint and bed elevation. The initial condition is the longitudinal profile in 2000. The coefficients  $C$  and  $D$  were influenced by bed shear stress. Due to the rapid increase in actual bed erosion rate after 2005, the parameters were adjusted

to match the actual changes. Before 2005,  $C$  was  $7.5 \text{ yr}^{-1}$ , and  $D$  was  $1.825 \text{ m}^2 \text{ yr}^{-1}$ . After 2005,  $C$  was  $36.5 \text{ yr}^{-1}$ , and  $D$  was  $9.125 \text{ m}^2 \text{ yr}^{-1}$ . The simulation was continued until 2017. The downstream boundary adopts the real bed change, while the upstream boundary condition is fixed, considering the dam is a fixed point. The bed is progressively scoured in the nearby downstream of the dam, and the knickpoint retreats and gradually fades away. The variation trend of the simulation and survey is generally consistent, includ-



**Figure 9.** Orthographic images (2000–2008), satellite image (2017), and flow paths of the studied reach of the Dajia River from 2000 to 2017.

ing the fact that intensive engineering works have been conducted in front of the dam to stabilize the bed.

#### 4 Discussion

Data on the changes in the riverbed, river width, and migration distance of the knickpoint for all three studied reaches are provided in Table 1. In addition, in Fig. 12a we use “*T*” symbols to represent the channel width (*W*) and depth (*D*) of the cross-sections in three study reaches. The aspect ratio (*W/D*) is labeled above every *T*. After the Chi-Chi earthquake, the channel geometry was not disturbed immediately. The aspect ratio of the Daan River exhibited only slight changes. Consequently, the aspect ratio significantly decreased with time from the downstream section. Subsequently, the aspect ratio recovered a little after 2011. The deepening of the upstream was slower than that downstream, but the later recovery was more obvious in the upstream area. The aspect ratio of the Zhuoshui River dramatically declined in the upstream part after construction of the Jiji Dam. This change extended gradually to the downstream section with time. In the Dajia River, owing to the combined effects of the upstream dam and the earthquake, channelization of the river started at both ends of the reach and then met in the middle. The examples of these three rivers allow us to deduce

the evolution of knickpoint retreat and transformation of the river pattern under the influence of dams and/or uplift.

The river pattern of knickpoint retreat is illustrated in Fig. 12b, and it was also observed in the Daan River. During the knickpoint retreat, the tool effect caused the river to narrow dramatically. However, after the river had reached a new equilibrium in a channelized pattern, the slope replacement resulted in a natural profile. The incision trend gradually slowed during the adjustment, and sedimentation may commence downstream (dashed line in Fig. 12b). The profile evolved from a concave curve to a graded profile (Chamberlin and Salisbury, 1904). In the case of the Daan River, the topography of the upstream gorge was gradually swept away, and the river pattern may be slowly restored to the original braided plain.

Before construction of the Jiji Dam, the studied reach of the Zhoushui River was a broad and braided river. The river armor layer was lost due to sediment trapping by the dam. Under the influence of the tool effect, the flow path in front of the dam gradually narrowed (Fig. 12c). The scouring boundary extended downstream of the dam. Because of the immovable knickpoint, the local slope at the dam toe became steeper, and the dam (acting as a non-erasable knickpoint) caused the river profile and sediment transport to remain at non-equilibrium.

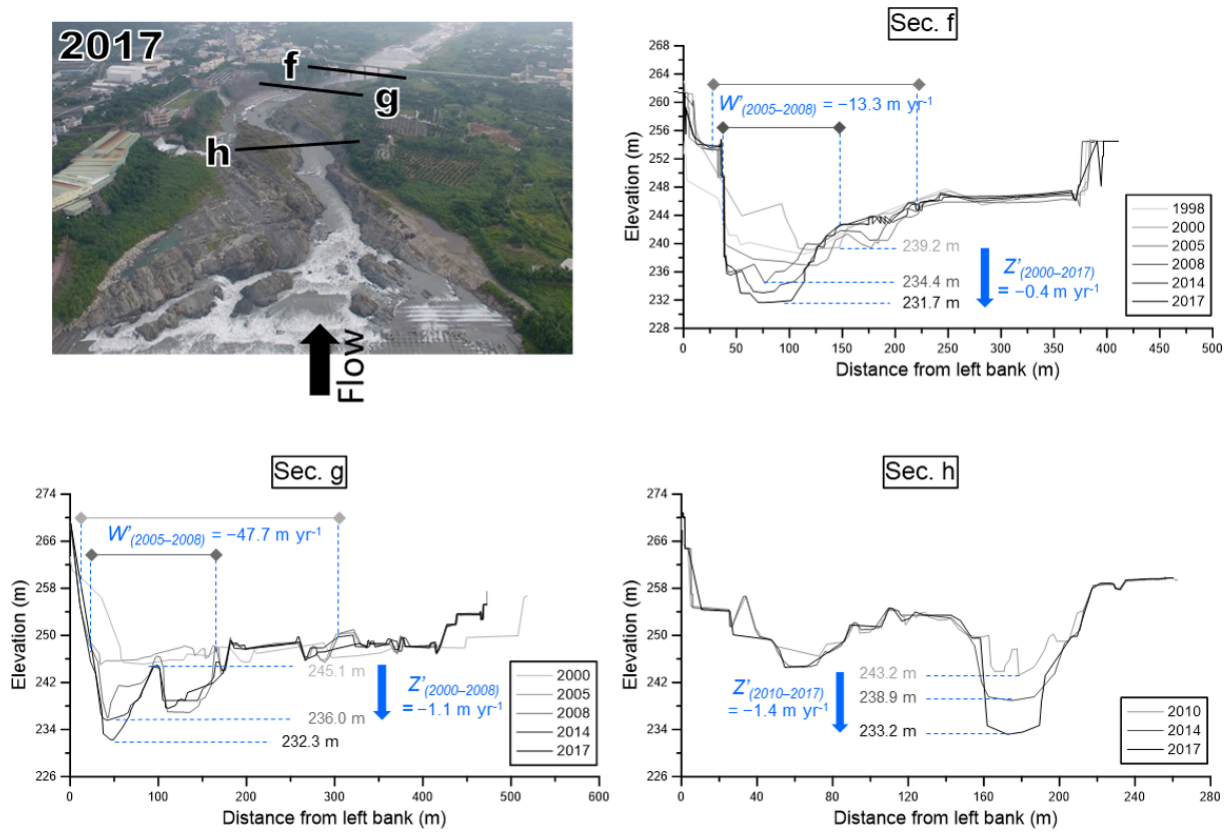


Figure 10. Cross-sections f–h of the Dajia River from 2000 to 2017 (from the WRA).

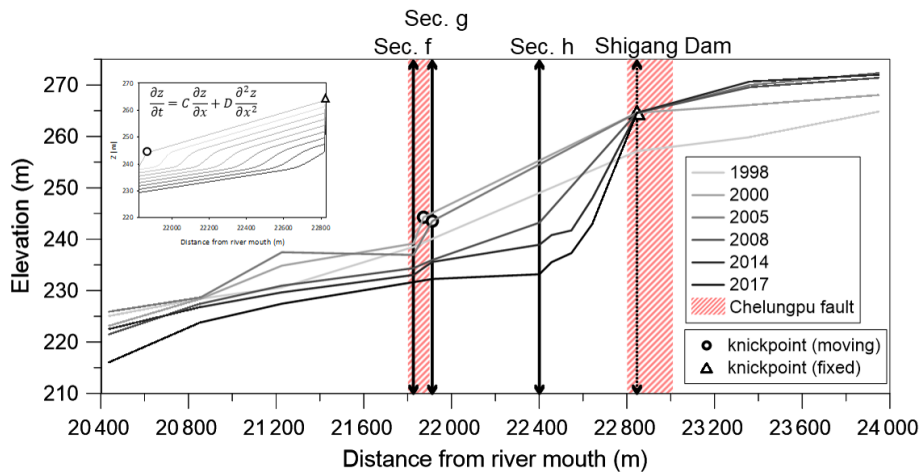
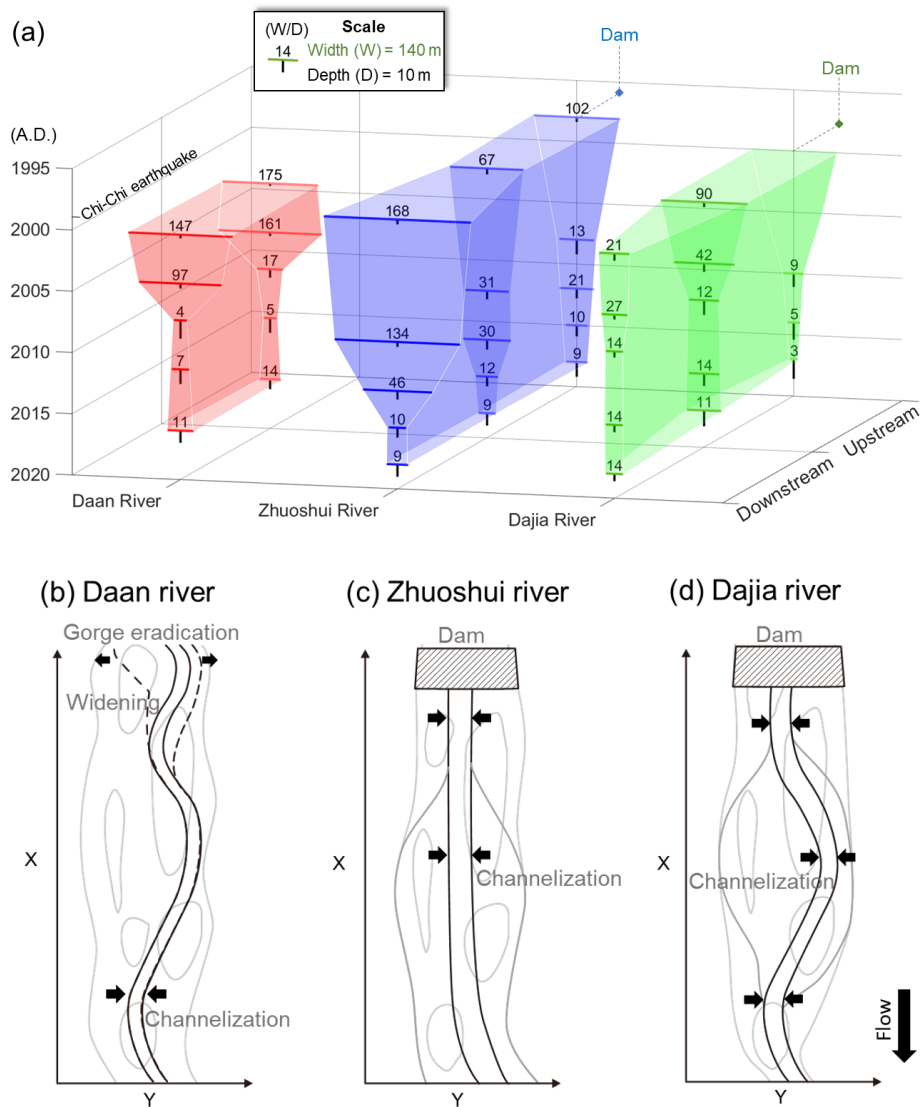


Figure 11. Longitudinal profiles of the studied reach of the Dajia River from 1998 to 2017 (from the WRA). Knickpoint retreats are simulated using the advective–diffusive model at the top left.

The reach downstream of the Shigang Dam on the Dajia River was simultaneously affected by coseismic uplift and the incision of a deep path in the soft rock in front of the dam. The knickpoint caused by fault uplift retreated upward with time. Although the uplift of the Dajia River was similar to that of the Daan River, the Shigang Dam (fixed point) re-

stricted knickpoint retreat in the Dajia River and led to scouring downward from the dam site. Therefore, we saw the river narrowing at the two ends of the affected reach and then progressively extending to the middle, as shown in Fig. 12d. The knickpoint caused by the earthquake was gradually removed,



**Figure 12.** (a) Channel width ( $W$ ), depth ( $D$ ), and aspect ratio ( $W/D$ ) of the studied reaches of the three rivers. The aspect ratio was defined as the ratio of the bankfull width to the depth of the bankfull channel. The vertical axis shows the time from 1995 downward to 2020, the horizontal axis shows the rivers, and the normal axis shows the sections from downstream to upstream. Schematic diagrams of knickpoint retreat and river pattern development for (b) coseismic uplift, (c) dam obstruction, and (d) dam obstruction and coseismic uplift.

but the effect of the dam remains. Therefore, the recovery of a braided river cannot happen in the Dajia River.

In Fig. 13, the discharge data of outflow from Shigang Dam (Dajia River) and Jiji Dam (Zhuoshui River) and the flow data of the Daan River from July 2005 to December 2019 are presented. The cumulative flow results show that the increasing trends in the discharge in the Dajia and Zhuoshui rivers are consistent. Both dams serve the purpose of controlling water levels for water supply and irrigation. The direct discharge is influenced by the variations in dry and rainy seasons, resulting in intermittent changes in the discharge. In contrast, the flow in the Daan River shows a continuous and stable increase. We observed a positive cor-

relation between the knickpoint retreat distances and the cumulative discharge in the Dajia and Daan rivers. However, the proportionality between discharge and knickpoint retreat rate in each river cannot be directly applied to another river (as evidenced by the comparison between the Dajia and Daan rivers). We speculate that this may be related to factors such as slope, river width, the elevation difference between the two river sections being a fixed point and a moving point, the protective engineering works under the Shigang Dam of the Dajia River, and local geology.

Overall, there are apparent differences in the morphological changes to rivers caused by natural and human factors. A knickpoint formed by fault-induced riverbed uplift is a

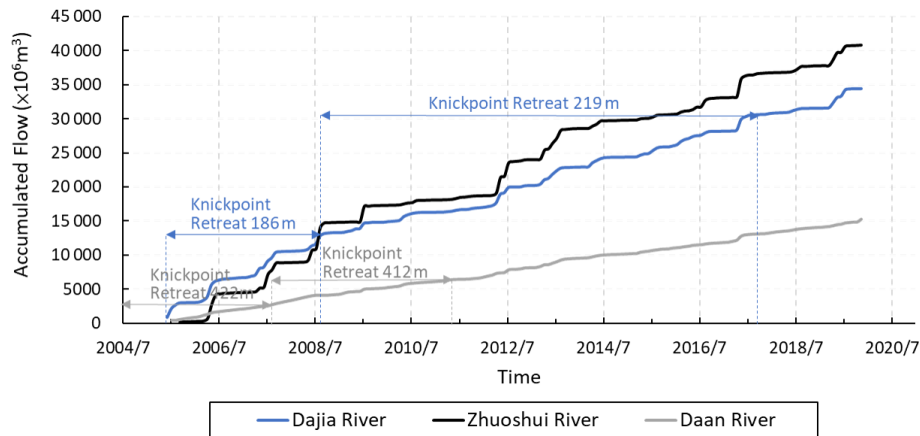


**Figure 13.** The cumulative flow in the three study reaches and the corresponding knickpoint retreat distances.

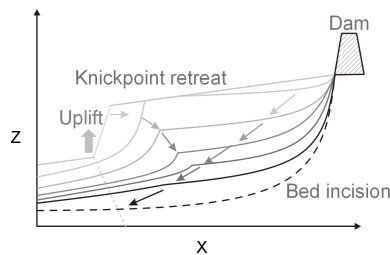


**Figure 14.** A schematic diagram of longitudinal profile development for the combined effects of dam construction and coseismic uplift.

moving point: as the knickpoint moves, the riverbed evolves gradually from an unstable state to an equilibrium. In contrast, a dam can be regarded as a fixed point on the river. The flow from the spillway outlet hits the riverbed continuously, which causes a decline in the erosion base level; therefore, downward erosion commences from the toe of the dam. For the case under the combined effect of fault uplift and dam obstruction, we inferred a schematic diagram of longitudinal profile development for the combined effects, as shown in Fig. 14. In Fig. 14, the uplift creates knickpoints that gradually retreat upstream. Meanwhile, starting from the dam toe, there is continuous deepening. When these two phenomena meet, changes resulting from natural tectonic movements of a riverbed may achieve equilibrium with time, whereas imbalance caused by anthropogenic structures may be enhanced with time.

## 5 Conclusions

The Daan River, Zhoushui River, and Dajia River in central Taiwan exhibited changes in river morphology after disturbances by earthquake uplift and dam obstruction during the past 20 years. The Daan River was affected by a thrust fault, the Zhoushui River was influenced by dam obstruction,

and the Dajia River was influenced by both the fault and a dam. In the Daan River, the greater slope accelerated the flow velocity and drove knickpoint retreat after removal of the armor layer, resulting in the progress of slope replacement. However, the incision faded with time, sediment deposition commenced, and the river showed potential for recovery to a braided river pattern. Because of sediment trapping by the Jiji Dam, the Zhoushui River has transformed from a braided river to a gorge river. The channelization started from the dam and expanded downward, and the incision progress caused the local slope at the toe to become steeper. Because the dam acts as an immovable knickpoint, the river's sediment equilibrium could not be re-established. The Shigang Dam on the Dajia River also caused a downward incision. The incision from the toe of the dam subsequently connected with the knickpoint retreat caused by headward erosion from downstream, forming a single, meandering channel at the front of the dam.

Knickpoints resulting from fault-induced riverbed uplift are moving points: as the knickpoint moves, the riverbed evolves gradually from an unstable state to an equilibrium state. In contrast, a dam, as a fixed point on the river, causes continuous degradation. When both effects exist on a reach, the impact of the knickpoint gradually fades away, but the effects of the dam on the river persist.

**Code availability.** The code, developed by the first author, includes the datasets used in the paper. However, as most of the data were obtained from third parties, we are unable to provide this as an open-access dataset. The code can be accessed upon request by contacting the author, and each request will be reviewed and processed on a case-by-case basis (contact email: hechen.tw@gmail.com).

**Data availability.** The data are stored at the respective universities of the authors. Since most of the data were obtained from third parties, we are unable to provide a complete open-access dataset.

However, data can be accessed upon request by contacting the authors. Each request will be reviewed and processed individually.

**Author contributions.** HEC was involved in methods development, modeling, data analysis, discussion, and paper preparation. YYC participated in data analysis, discussion, and paper preparation. CYC conducted the field survey and collected and analyzed data. SCC contributed to the preparation of the hypothesis, concept, research design, and conclusions and to the writing of the paper.

**Competing interests.** The contact author has declared that none of the authors has any competing interests.

**Disclaimer.** Publisher's note: Copernicus Publications remains neutral with regard to jurisdictional claims made in the text, published maps, institutional affiliations, or any other geographical representation in this paper. While Copernicus Publications makes every effort to include appropriate place names, the final responsibility lies with the authors.

**Acknowledgements.** The Ministry of Science and Technology, Taiwan, partially supported this research under grant no. 111-2625-M-005-001. The authors would like to thank AFASI, MOST, and CSRSR/NCU for supplying satellite imagery data and the WRA for supplying river measurement data.

**Review statement.** This paper was edited by Tom Coulthard and reviewed by three anonymous referees.

## References

- Ahmed, M. F., Rogers, J. D., and Ismail, E. H.: Knickpoints along the upper Indus River, Pakistan: an exploratory survey of geomorphic processes, *Swiss J. Geosci.*, 111, 191–204, <https://doi.org/10.1007/s00015-017-0290-3>, 2018.
- Bishop, P., Hoey, T. B., Jansen, J. D., and Artza, I. L.: Knickpoint recession rate and catchment area: the case of uplifted rivers in Eastern Scotland, *Earth Surf. Proc. Land.*, 30, 767–778, <https://doi.org/10.1002/esp.1191>, 2005.
- Braatne, J. H., Rood, S. B., Goater, L. A., and Blair, C. L.: Analyzing the impacts of dams on riparian ecosystems: a review of research strategies and their relevance to the Snake River through Hells Canyon, *Environ. Manage.*, 41, 267–281, <https://doi.org/10.1007/s00267-007-9048-4>, 2008.
- Brandt, S. A.: Classification of geomorphological effects downstream of dams, *Catena*, 40, 375–401, [https://doi.org/10.1016/S0341-8162\(00\)00093-X](https://doi.org/10.1016/S0341-8162(00)00093-X), 2000.
- Bressan, F., Papanicolaou, A. N., and Abban, B.: A model for knickpoint migration in first- and second-order streams, *Geophys. Res. Lett.*, 41, 4987–4996, <https://doi.org/10.1002/2014GL060823>, 2014.
- Chamberlin, T. C. and Salisbury, R. D.: *Geology: Geologic processes and their results*, H. Holt, ISBN 10:1022257498, ISBN 13:978-1022257498, 1904.
- Choi, S. U., Yoon, B., and Woo, H.: Effects of dam-induced flow regime change on downstream river morphology and vegetation cover in the Hwang River, Korea, *River Res. Appl.*, 21, 315–325, <https://doi.org/10.1002/rra.849>, 2005.
- Clark, M. K., Maheo, G., Saleeby, J., and Farley, K. A.: The non-equilibrium landscape of the southern Sierra Nevada, California, *GSA Today*, 15, 4–10, [https://doi.org/10.1130/1052-5173\(2005\)015\[4:TNLOTS\]2.0.CO;2](https://doi.org/10.1130/1052-5173(2005)015[4:TNLOTS]2.0.CO;2), 2005.
- Cook, K. L., Turowski, J. M., and Hovius, N.: A demonstration of the importance of bedload transport for fluvial bedrock erosion and knickpoint propagation, *Earth Surf. Proc. Land.*, 38, 683–695, <https://doi.org/10.1002/esp.3313>, 2013.
- Cook, K. L., Turowski, J. M., and Hovius, N.: River gorge eradication by downstream sweep erosion, *Nat. Geosci.*, 7, 682–686, <https://doi.org/10.1038/ngeo2224>, 2014.
- Crosby, B. T., and Whipple, K. X.: Knickpoint initiation and distribution within fluvial networks: 236 waterfalls in the Waipaoa River, North Island, New Zealand, *Geomorphology*, 82, 16–38, <https://doi.org/10.1016/j.geomorph.2005.08.023>, 2006.
- Dotterweich, M.: The history of soil erosion and fluvial deposits in small catchments of central Europe: deciphering the long-term interaction between humans and the environment – a review, *Geomorphology*, 101, 192–208, <https://doi.org/10.1016/j.geomorph.2008.05.023>, 2008.
- Engelund, F.: Instability of erodible beds, *J. Fluid Mech.*, 42, 225–244, <https://doi.org/10.1017/S0022112070001210>, 1970.
- Exner, F. M.: Über die Wechselwirkung zwischen Wasser und Geschiebe in Flüssen, *Sitzungber. Acad. Wissenschaften Wien Math. Naturwiss.*, 134, 165–180, 1925.
- Gardner, T. W.: Experimental study of knickpoint and longitudinal profile evolution in cohesive, homogeneous material, *Geol. Soc. Am. Bull.*, 94, 664–672, 1983.
- Graf, W. L.: Downstream hydrologic and geomorphic effects of large dams on American rivers, *Geomorphology*, 79, 336–360, <https://doi.org/10.1016/j.geomorph.2006.06.022>, 2006.
- Hayakawa, Y. S., Matsuta, N., and Matsukura, Y.: Rapid recession of fault-scarp waterfalls: Six-year changes following the 921 Chi-Chi Earthquake in Taiwan, *Chikei/Transactions, Japanese Geomorphological Union*, 30, 1–13, 2009.
- Heijnen, M. S., Clare, M. A., Cartigny, M. J. B., Talling, P. J., Hage, S., Lintern, D. G., Stacey, C., Parsons, D. R., Simmons, S. M., Chen, Y., Sumner, E. J., Dix, J. K., and Hughes Clarke, J. E.: Rapidly-migrating and internally-generated knickpoints can control submarine channel evolution, *Nat. Commun.*, 11, 3129–3129, <https://doi.org/10.1038/s41467-020-16861-x>, 2020.
- Hoffmann, T.: Sediment residence time and connectivity in non-equilibrium and transient geomorphic systems, *Earth-Sci. Rev.*, 150, 609–627, <https://doi.org/10.1016/j.earscirev.2015.07.008>, 2015.
- Holland, W. N., and Pickup, G.: Flume study of knickpoint development in stratified sediment, *Geol. Soc. Am. Bull.*, 87, 76–82, [https://doi.org/10.1130/0016-7606\(1976\)87<76:FSOKDI>2.0.CO;2](https://doi.org/10.1130/0016-7606(1976)87<76:FSOKDI>2.0.CO;2), 1976.
- Horn, J. D., Joeckel, R. M., and Fielding, C. R.: Progressive abandonment and planform changes of the central Platte River in Nebraska, central USA, over his-



- torical timeframes, *Geomorphology*, 139, 372–383, <https://doi.org/10.1016/j.geomorph.2011.11.003>, 2012.
- Howard, A. D., Dietrich, W. E., and Seidl, M. A.: Modeling fluvial erosion on regional to continental scales, *J. Geophys. Res.*, 99, 971–986, <https://doi.org/10.1029/94jb00744>, 1994.
- Huang, M.-W., Pan, Y.-W., and Liao, J.-J.: A case of rapid rock riverbed incision in a coseismic uplift reach and its implications, *Geomorphology*, 184, 98–110, <https://doi.org/10.1016/j.geomorph.2012.11.022>, 2013.
- Huang, M. W., Liao, J. J., Pan, Y. W., and Cheng, M. H.: Rapid channelization and incision into soft bedrock induced by human activity – Implications from the Bachang River in Taiwan, *Eng. Geol.*, 177, 10–24, <https://doi.org/10.1016/j.enggeo.2014.05.002>, 2014.
- Inbar, M.: Effect Of Dams On Mountainous Bedrock Rivers, *Phys. Geogr.*, 11, 305–319, <https://doi.org/10.1080/02723646.1990.10642409>, 1990.
- Kingsford, R. T.: Ecological impacts of dams, water diversions and river management on floodplain wetlands in Australia, *Aust. Ecol.*, 25, 109–127, <https://doi.org/10.1046/j.1442-9993.2000.01036.x>, 2000.
- Kong, D., Latrubesse, E. M., Miao, C., and Zhou, R.: Morphological response of the Lower Yellow River to the operation of Xiaolangdi Dam, China, *Geomorphology*, 350, 106931–106931, <https://doi.org/10.1016/j.geomorph.2019.106931>, 2020.
- Kuo, C.-W., Tfwala, S., Chen, S.-C., An, H.-P., and Chu, F.-Y.: Determining transition reaches between torrents and downstream rivers using a valley morphology index in a mountainous landscape, *Hydrol. Process.*, 35, e14393, <https://doi.org/10.1002/hyp.14393>, 2021.
- Lai, Y. G., Greimann, B. P., and Wu, K.: Soft Bedrock Erosion Modeling with a Two-Dimensional Depth-Averaged Model, *J. Hydraul. Eng.*, 137, 804–814, [https://doi.org/10.1061/\(asce\)hy.1943-7900.0000363](https://doi.org/10.1061/(asce)hy.1943-7900.0000363), 2011.
- Lang, A., Bork, H., Mäkel, R., Preston, N., Wunderlich, J., and Dikau, R.: Changes in sediment flux and storage within a fluvial system: some examples from the Rhine catchment, *Hydrol. Process.*, 17, 3321–3334, <https://doi.org/10.1002/hyp.1389>, 2003.
- Lee, J. C., Chu, H. T., Angelier, J., Chan, Y. C., Hu, J. C., Lu, C. Y., and Rau, R. J.: Geometry and structure of northern surface ruptures of the 1999  $M_w = 7.6$  Chi-Chi Taiwan earthquake: Influence from inherited fold belt structures, *J. Struct. Geol.*, 24, 173–192, [https://doi.org/10.1016/S0191-8141\(01\)00056-6](https://doi.org/10.1016/S0191-8141(01)00056-6), 2002.
- Leopold, L. B. and Wolman, M. G.: River channel patterns: braided, meandering, and straight, US Government Printing Office, <https://doi.org/10.3133/pp282B>, 1957.
- Lin, A., Ouchi, T., Chen, A., and Maruyama, T.: Co-seismic displacements, folding and shortening structures along the Chelungpu surface rupture zone occurred during the 1999 Chi-Chi (Taiwan) earthquake, *Tectonophysics*, 330, 225–244, [https://doi.org/10.1016/S0040-1951\(00\)00230-4](https://doi.org/10.1016/S0040-1951(00)00230-4), 2001.
- Liro, M.: Dam-induced base-level rise effects on the gravel-bed channel planform, *Catena*, 153, 143–156, <https://doi.org/10.1016/j.catena.2017.02.005>, 2017.
- Liro, M.: Dam reservoir backwater as a field-scale laboratory of human-induced changes in river biogeomorphology: A review focused on gravel-bed rivers, *Sci. Total Environ.*, 651, 2899–2912, <https://doi.org/10.1016/j.scitotenv.2018.10.138>, 2019.
- Lyell Sir, C. and Deshayes, G. P.: Principles of geology; being an attempt to explain the former changes of the earth's surface, by reference to causes now in operation, J. Murray, London, ISBN 10:1108001351, ISBN 13:978-1108001359, 1830.
- Magilligan, F. J. and Nislow, K. H.: Changes in hydrologic regime by dams, *Geomorphology*, 71, 61–78, <https://doi.org/10.1016/j.geomorph.2004.08.017>, 2005.
- Merritts, D. and Vincent, K. R.: Geomorphic response of coastal streams to low, intermediate, and high rates of uplift, Medocino triple junction region, northern California, *GSA Bull.*, 101, 1373–1388, [https://doi.org/10.1130/0016-7606\(1989\)101<1373:GROCST>2.3.CO;2](https://doi.org/10.1130/0016-7606(1989)101<1373:GROCST>2.3.CO;2), 1989.
- Nelson, N. C., Erwin, S. O., and Schmidt, J. C.: Spatial and temporal patterns in channel change on the Snake River downstream from Jackson Lake dam, Wyoming, *Geomorphology*, 200, 132–142, <https://doi.org/10.1016/j.geomorph.2013.03.019>, 2013.
- Olsen, N. R. B.: Two-dimensional numerical modelling of flushing processes in water reservoirs, *J. Hydraul. Res.*, 37, 3–16, <https://doi.org/10.1080/00221689909498529>, 1999.
- Ota, Y., Chen, Y.-G., and Chen, W.-S.: Review of paleoseismological and active fault studies in Taiwan in the light of the Chichi earthquake of September 21, 1999, *Tectonophysics*, 408, 63–77, <https://doi.org/10.1016/j.tecto.2005.05.040>, 2005.
- Petts, G. E. and Gurnell, A. M.: Dams and geomorphology: research progress and future directions, *Geomorphology*, 71, 27–47, <https://doi.org/10.1016/j.geomorph.2004.02.015>, 2005.
- Seidl, M. A. and Dietrich, W. E.: The problem of channel erosion into bedrock, *Funct. Geomorphol.*, 23, 101–124, 1992.
- Shafroth, P. B., Perry, L. G., Rose, C. A., and Braatne, J. H.: Effects of dams and geomorphic context on riparian forests of the Elwha River, Washington, *Ecosphere*, 7, e01621–e01621, <https://doi.org/10.1002/ecs2.1621>, 2016.
- Słowik, M., Dezső, J., Marciniak, A., Tóth, G., and Kovács, J.: Evolution of river planforms downstream of dams: Effect of dam construction or earlier human-induced changes?, *Earth Surf. Proc. Land.*, 43, 2045–2063, <https://doi.org/10.1002/esp.4371>, 2018.
- Surian, N. and Rinaldi, M.: Morphological response to river engineering and management in alluvial channels in Italy, *Geomorphology*, 50, 307–326, [https://doi.org/10.1016/S0169-555X\(02\)00219-2](https://doi.org/10.1016/S0169-555X(02)00219-2), 2003.
- Tomkin, J. H., Brandon, M. T., Pazzaglia, F. J., Barbour, J. R., and Willett, S. D.: Quantitative testing of bedrock incision models for the Clearwater River, NW Washington State, *J. Geophys. Res.-Solid*, 108, 2308, <https://doi.org/10.1029/2001jb000862>, 2003.
- Whipple, K. X.: Fluvial landscape response time: how plausible is steady-state denudation?, *Am. J. Sci.*, 301, 313–325, <https://doi.org/10.2475/ajs.301.4-5.313>, 2001.
- Whipple, K. X.: Bedrock Rivers And The Geomorphology Of Active Orogens, *Annu. Rev. Earth Planet. Sci.*, 32, 151–185, <https://doi.org/10.1146/annurev.earth.32.101802.120356>, 2004.
- Whipple, K. X. and Tucker, G. E.: Dynamics of the stream-power river incision model: Implications for height limits of mountain ranges, landscape response timescales, and research needs, *J. Geophys. Res.-Solid*, 104, 17661–17674, <https://doi.org/10.1029/1999jb900120>, 1999.
- Whipple, K. X. and Tucker, G. E.: Implications of sediment-flux-dependent river incision models for landscape evolu-

- tion, *J. Geophys. Res.-Solid*, 107, ETG 3-1–ETG 3-20, <https://doi.org/10.1029/2000JB000044>, 2002.
- Williams, G. P. and Wolman, M. G.: Downstream effects of dams on alluvial rivers, US Government Printing Office, 1286, <https://doi.org/10.3133/pp1286,1984>, 1984.
- Zhou, M., Xia, J., Deng, S., Lu, J., and Lin, F.: Channel adjustments in a gravel-sand bed reach owing to upstream damming, *Global Planet. Change*, 170, 213–220, <https://doi.org/10.1016/j.gloplacha.2018.08.014>, 2018.